Peer-reviewed version available at *Genes* **2020**, *11*, 1030; doi:10.3390/genes11091030

Article

Biomarkers, Master Regulators and Genomic Fabric Remodeling in a Case of Papillary Thyroid Carcinoma

Dumitru A Iacobas [1]*

[1] Personalized Genomics Laboratory, CRI Center for Computational Systems Biology, Roy G Perry College of Engineering, Prairie View A&M University, Prairie View, TX 77446; daiacobas@pvamu.edu

* Correspondence: daiacobas@pvamu.edu; Tel.: +1 (936) 261-9926

Abstract: Publically available (own) transcriptomic data were re-analyzed to quantify the alteration of functional pathways in the thyroid cancer, establish the gene hierarchy, identify potential gene targets and predict the effects of their manipulation. The expression data were generated from one case of papillary thyroid carcinoma (PTC) and from genetically manipulated BCPAP (papillary) and 8505C (anaplastic) human thyroid cancer cell lines. The study used the genomic fabric perspective that considers the transcriptome as a multi-dimensional mathematical object based on the three independent characteristics that can be derived for each gene from the expression data. We found remarkable remodeling of the thyroid hormone synthesis, cell cycle, oxidative phosphorylation and apoptosis pathways. Serine peptidase inhibitor, Kunitz type, 2 (*SPINT2*) was identified as the Gene Master Regulator of the investigated PTC. The substantial increase of the expression synergism of *SPINT2* with apoptosis genes in the cancer nodule with respect to the surrounding normal tissue (NOR) suggests that its experimental overexpression may force the PTC cells into apoptosis with negligible effect on the NOR cells. The predictive value of the expression coordination for the expression regulation was validated with data from 8505C and BCPAP cells before and after lentiviral transfection with *DDX19B*.

Keywords: 8505C cell line; apoptosis; BCPAP cell line; CFLAR, DDX19B; IL6; oxidative phosphorylation; SPINT2; thyroid hormone synthesis; weighted pathway regulation.

1. Introduction

Much less lethal and much less frequent than other malignancies, thyroid cancer (**TC**) in the U.S.A. is expected to add in 2020 new 52,440 cases (12,270 men and 40,170 women). Although TC affects over three times more women than men, the number of death (2,180) is practically equally distributed between the two sexes (1,040 men and 1,140 women) [1]. There are four major types of thyroid cancers: papillary (here after denoted as **PTC**, 70-80% of total cases), follicular (**FTC**, 10-15%), medullary (**MTC**, ~2%) and anaplastic (**APC**, ~2%). PTC and MTC exhibit well differentiated cells and are treatable, while APC is undifferentiated and (for now) untreatable [2].

Considerable effort has been done in the last decades to identify DNA mutations and the oncogenes (whose turn on) and tumor suppressor factors (whose turn off) are responsible for triggering TC. The 25.0 release (May 07, 2020) of the Genomic Data Commons Data Portal [3] includes 11,128 confirmed mutations detected on 13,564 genes sequenced from 1,440 (553 male and 887 female) cases of thyroid cancers. The most frequently mutated gene reported in the portal is: *BRAF* (B-Raf proto-oncogene, serine/ threonine kinase) with up to 10 mutations identified in 20.56% of cases. Far down as mutation frequency are: *NRAS* (neuroblastoma RAS viral (v-ras) oncogene

homolog) with 2 mutations in 2.71% of cases, *TTN* (titin), total 40 mutations in 2.29% of cases and *TG* (thyroglobulin), total 26 mutations in 1.67% of cases [3]. For most genes, the portal [3] shows the specific types and locations of the mutations and the diseases they were found associated with. However, a particular form of cancer is associated with numerous mutated genes and a particular mutated gene can be found in several forms of cancer. How many mutations one needs to identify to decide upon the right form of cancer? Are there exclusive combinations of mutations for a particular form of cancer and only for that form? If they are, the number of the implicated genes should be large enough to avoid any overlap with other form of cancer. Although the incidence of each particular mutation in the explored cohort of patients is known, it is impossible to determine the predictive values of such combinations because, for more than 3 mutations, the number of possibilities ($\geq 2.3 \times 10^{11}$) exceeds the human population of the Earth. Even though one can determine via conditioned probabilities (actual conditioned frequencies) what is the chance to find the same combination of (few) mutations in other persons, the diagnostic value is very poor. And let us not forget that the mutations were identified with respect to a reference human genome representing the perfectly healthy individual regardless of race, sex, age, environmental conditions etc.

There are several commercially available gene assays used for preoperative diagnostic and classification of TCs (e.g.: [4,5]). Recently, Foundation Medicine [6] compiled a list of 310 genes with full coding exonic regions for the detection of substitutions, insertion-deletions and copy-number alterations. An additional list of the same Foundation contains 36 genes with intronic regions useful for the detection of gene rearrangements (one gene with a promoter region and one non-coding RNA gene) [6]. For all these assays, the question is how many and what genes should be mutated/regulated to assign a particular diagnostic? Most importantly, how they determined the predictive values of each combination of genes. In [6], there are 346 combinations of one gene, 59,685 of two, 6,843,880 combinations of three, 587 mil of four and over 40 bln of five and more. Therefore, for practical purposes, only the most relevant one or two biomarkers are currently used that considerably limits the diagnostic accuracy.

If the diagnostic value of mutations and/or regulations is doubtful, what about their use for therapeutic purposes? Is restoring the normal sequence/expression level of one biomarker enough to cure the cancer? Considering that the "trusted" biomarkers were selected from the genes with the most frequently altered sequence and/or expression level, it means that they are less protected by the cellular homeostatic mechanisms, like minor players. The cell is supposed to invest energy to protect the sequence and expression of genes critical for their survival, proliferation and integration in multicellular structures. As such, biomarker(s)' restoration may have little consequence for the cancer cells.

While we don't see for now a genomic solution for the cancer diagnostic, we believe that our Gene Master Regulators (**GMR**) approach [7,8] is a reasonable alternative to the actual biomarker oriented gene therapy. The GMR of a particular cell phenotype is the gene whose highly protected sequence/expression by the cellular homeostatic mechanisms regulates major functional pathways through expression coordination with their genes. Since, as we proved recently [7-9], the GMR of the cancer nodule performs poorly in the surrounding cancer-free tissue of the tumor, then, manipulating the GMR's expression is expected to selectively destroy cancer cells with little consequences on the normal ones.

In this study, we reanalyze previously published transcriptomic data to quantify the cancer-related remodeling of major functional pathways in the PTC nodule with respect to the cancer-free resection margins (**NOR**) of a surgically removed tumor. The Gene Commanding Height (**GCH**) hierarchy and the GMRs are determined in both PTC and NOR, and the potential regulations of the apoptosis genes in response to the GMR manipulation are predicted. The GCH scores of the top genes are compared to those of the most mutated genes in TC as well as of the considered cancer biomarkers. Transcriptomic profiles of two standard thyroid cancer cell lines before and after stably transfection with a gene (*DDX19B*) are used to determine the predictive value of the coordination analysis in untreated cells for the regulation in treated ones.

2. Materials and Methods

2.1. Gene expression data

We reanalyze transcriptomic data from one case of papillary carcinoma, pathological stage pT3NOMx, deposited in the Gene Expression Omnibus (GEO) of the National Center for Biotechnology Information (NCBI) [10] as GSE97001 and reported in previous publications [7,8]. In the preceding studies, the four quarters of the most homogeneous 20mm^3 part of the frozen unilateral, single, 32.0 mm PTC nodule and four small pieces from the NOR of the same gland from the same patient were profiled separately. Expression data were normalized iteratively to the median of all quantifiable genes in all samples and the transcript abundances expressed as multiples of the average expression level of the median gene in each region. Transcriptomic data from this surgically removed tumor were compared to the gene expression profiles of two standard human thyroid cancer cell lines: **BCPAP** (papillary) and **8505C** (anaplastic) deposited as GSE97002. Moreover, in order to justify the predictive value of the coordination analysis, we have used the gene expression profiles of these two cell lines after stable lentiviral transfection with DEAD (Asp-Glu-Ala-Asp) box polypeptide 19B *(DDX19B*) deposited as GSE97028.

2.2. Single-gene transcriptomic quantifiers

2.2.1. Biological replicas, profiling redundancy and average expression level

The four-biological replicas experimental design provided for every single gene in each region three independent measures: i) average expression level, ii) expression variation and iii) expression coordination with each other gene [11]. We utilized these three measures and combinations of them to establish the gene hierarchies and characterize the contribution of each gene to the cancer-related reorganization of the thyroid transcriptome.

The Agilent two-color expression microarrays used in the re-analyzed experiments probed redundantly the genes with various number of spots from 1 to 20 as for *MIEF1* (mitochondrial elongation factor 1) and *SRRT* (serrate, RNA effector molecule). Therefore, for each gene "*i*", we computed the average expression level over the group of R_i spots probing redundantly the same transcript of the average expression levels measured by spot "*k*" across the biological replicas.

$$\mu_i^{(NOR/PTC)} = \frac{1}{R_i}\sum_{k=1}^{R_i}\mu_{i,k}^{(NOR/PTC)} = \frac{1}{R_i}\sum_{k=1}^{R_i}\left(\frac{1}{4}\sum_{j=1}^{4}a_{i,k,j}^{(NOR/PTC)}\right) \quad , \quad where: \tag{1}$$

$a_{i,k,j}^{(NOR/PTC)}$ = expression level of gene "*i*" probed by spot "*k*" on biological replica "*j*"

2.2.2. Expression variation

Because of the probing redundancy, instead of the coefficient of variation (**CV**) we used the *Relative Expression Variability* (**REV**), a Bonferroni-like corrected mid-interval of the chi-square estimate of the pooled CV for all quantifiable transcripts of the same gene [12]:

$$REV_i^{(NOR/PTC)} = \frac{1}{2}\left(\underbrace{\sqrt{\frac{r_i}{\chi^2(r_i;0.975)}}}_{\text{correction coefficient}} + \sqrt{\frac{r_i}{\chi^2(r_i;0.025)}}\right)\underbrace{\sqrt{\frac{1}{R_i}\sum_{k=1}^{R_i}\left(\frac{s_{ik}^{(NOR/PTC)}}{\mu_{ik}^{(NOR/PTC)}}\right)^2}}_{\text{pooled CV}} \times 100\% \tag{2}$$

μ_{ik} = average expression level of gene i probed by spot k (= 1, ..., R_i) in the 4 biological replicas

s_{ik} = standard deviation of the expression level of gene i probed by spot k

$r_i = 4R_i - 1 =$ number of degrees of freedom

R_i = number of microarray spots probing redundantly gene *i*

Lower *REV* indicates stronger control by the cellular homeostatic mechanisms to limit the expression fluctuations, expected for genes critical for survival, proliferation and phenotypic expression. Therefore, we use also the *Relative Expression Control* (***REC***):

$$REC_i^{(NOR,PTC)} \equiv \frac{\langle REV \rangle^{(NOR/PTC)}}{REV_i^{(NOR/PTC)}} - 1 \quad (3)$$

$\langle\ \rangle$ = median for all genes profiled in that phenotype

As defined, positive *RECs* point out to genes that are more controlled than the median while negative *RECs to* less controlled genes in that phenotype. It is natural to assume that the cell invests more energy to control the expressions of more important genes for its survival, phenotypic expression and integration into multi-cellular structure. As such, *REC* is a major factor to consider in establishing the gene hierarchy.

2.2.3. Expression coordination

The expression coordination of two genes in the same region was quantified by their pair-wise momentum-product Pearson correlation coefficient between the two sets of expression levels across biological replicas, " $\rho_{ij}^{(NOR/PTC)}$ ". The statistical significance was evaluated with the two-tail *t*-test for the degrees of freedom df = 4(biological replicas)*R (number of spots probing redundantly each of the correlated transcripts) − 2. Two genes were considered as synergistically expressed (positive coordination) if their expression levels fluctuate in phase across biological replicas. They are considered as antagonistically expressed (negative coordination) when their expression levels manifest opposite tendencies and independently expressed (neutral coordination) when the expression fluctuations of one gene are not related to the fluctuations of the other [12].

We computed also the coordination power $CP_{i,\Gamma}^{(NOR/PTC)}$ [13] and the Overall Coordination $OC_{i,\Gamma}^{(NOR/PTC)}$ of a gene "*i*" with respect to the functional pathway "*Γ*" in each of the two profiled regions (NOR and PTC):

$$CP_{i,\Gamma}^{(NOR/PTC)} \equiv \overline{\rho_{ij}^{(NOR/PTC)}}\Big|_{\forall j\in\Gamma, j\neq i} \times 100\% \quad , \quad OC_{i,\Gamma}^{(NOR/PTC)} \equiv \exp\left(\frac{4}{N}\sum_{j\in\Gamma, j\neq i}\rho_{ij}^2 - 1\right) \quad (4)$$

Both $CP_{i,\Gamma}^{(NOR/PTC)}$ and $OC_{i,\Gamma}^{(NOR/PTC)}$ are measures of the gene "*i*" influence on "*Γ*"

2.3. Gene Commanding Height (GCH) and Gene Master Regulator (GMR)

In previous papers [7-9], we introduced the Gene Commanding Height (**GCH**), a combination of the expression control and expression coordination with all (ALL) other genes, to establish the gene hierarchy in each phenotype:

$$GCH_i^{(NOR,PTC)} \equiv \left(REC_i^{(NOR,PTC)} + 1\right) OC_{i,ALL}^{(NOR/PTC)} \equiv \frac{\langle REV \rangle^{(NOR/PTC)}}{REV_i^{(NOR/PTC)}} \exp\left(\frac{4}{N}\sum_{j\in ALL, j\neq i}\rho_{ij}^2 - 1\right) \quad (5)$$

The top gene (highest GCH) in each phenotype was termed Gene Master Regulator (**GMR**) of that phenotype. The very strict control of the GMR expression indicates that is utterly important for the cell survival and the very high overall coordination suggests how much its expression regulates the expressions of many other genes.

2.4. Expression regulation

A gene was considered as significantly regulated in the PTC with respect to the NOR if the absolute expression ratio exceeds the cut-off (CUT) value computed individually for each gene by considering the expression variabilities of that gene in both compared conditions [9].

$$\left|x_i^{(NOR\to PTC)}\right| > CUT_i = 1+\frac{1}{100}\sqrt{2\left(\left(REV_i^{(NOR)}\right)^2+\left(REV_i^{(PTC)}\right)^2\right)} \quad , \quad where:$$

$$x_i \equiv \begin{cases} \dfrac{\mu_i^{(PTC)}}{\mu_i^{(NOR)}} & , \text{ if } \mu_i^{(PTC)} > \mu_i^{(NOR)} \\ -\dfrac{\mu_i^{(NOR)}}{\mu_i^{(PTC)}} & , \text{ if } \mu_i^{(PTC)} < \mu_i^{(NOR)} \end{cases} \quad , \quad \mu_i^{(PTC/NOR)} = \frac{1}{R_i}\sum_{k=1}^{R_i}\mu_{ik}^{(PTC/NOR)} \tag{6}$$

The "CUT" criterion for individual genes eliminates the false positives and the false negatives selected by considering an uniform absolute fold-change cut-off (e.g. 1.5x). In addition to the percentage of up- and down-regulated genes (that considers all genes as equal contributors to the alteration of a pathway), or the expression ratios "*x*", we prefer the Weighted Individual (gene) Regulation [14], "*WIR*":

$$WIR_i^{(NOR\to PTC)} \equiv \mu_i^{(NOR)}\frac{x_i}{|x_i|}\left(|x_i|-1\right)\left(1-p_i\right) \quad where:$$

$$\mu_i^{(NOR)} = \text{average expression in the normal tissue,} \tag{7}$$

$$p_i = \text{p-value of the regulation}$$

Note in equation (7) that WIR takes into account the normal expression of that gene (i.e. in NOR), its expression ratio (PTC vs NOR) and the confidence interval (1-p) of the regulation.

2.4. Quantifiers of the functional genomic fabrics

The Kyoto Encyclopedia of Genes and Genomes [15,16] was used to select the genes involved in the thyroid hormone synthesis (**THS**), cell cycle (**CC**) and oxidative phosphorylation (**OPH**), as well as how experimental manipulation of the PTC GMR regulates the programmed cell death (apoptosis, **APO**).

Median REC over a gene selection (e.g. apoptosis pathway) was used to compare the expression controls of that selection in in different regions or two different gene selections in the same region. Alteration of the genomic fabrics was quantified by the average "*X*" of the absolute expression ratios and by the average "*WPR*" (Weighted Pathway Regulation) of the absolute *WIR*s over a particular "selection" of genes:

$$X_{selection}^{(NOR\to PTC)} \equiv \overline{\left|x_i^{(NOR\to PTC)}\right|}_{\forall i\in selection}$$

$$WPR_{selection}^{(NOR\to PTC)} \equiv \overline{\left|WIR_i^{(NOR\to PTC)}\right|}_{\forall i\in selection} \tag{8}$$

3. Results

3.1. Overall results

14,903 well-quantified unigenes in all PTC and NOR samples, and in BCPAP and 8505C cells were considered in the sequent analyses (the groups probing redundantly the same transcript were replaced by their averages in each biological replica). Eukaryotic translation elongation factor 1 alpha 1 (*EEF1A1*) had the largest expression (82.31 median gene expression units) in NOR (not significantly regulated in PTC). Niemann-Pick disease, type C2 (*NPC2*) had the largest expression in PTC (86.97 median gene expression units), up-regulated by 7.24x with respect to NOR. Notch 1 (*NOTCH1*) with 82.35 had the largest expression in the BCPAP cells and myelin protein zero-like 3 (*MPZL3*) with 107.60 tops the gene expression level in the 8505C cells.

Out of the quantified unigenes, 1,225 (8.22%) were down-regulated and 1,852 (12.42%) were up-regulated in PTC with respect to NOR. The average absolute expression ratio for all genes was *X*

= 1.768 (median |x| = 1.309) and the *WPR* was 1.071 (median WIR = 0.046). Chitinase 3-like 1 (*CHI3L1*) was the most up-regulated (x = 219.38) and trefoil factor 3 (intestinal) (*TFF3*) the most down-regulated (x-99.86) gene in PTC.

3.2. Three independent measures for each gene

Figure 1 illustrates the independence of the three measures for the first 50 alphabetically ordered gene involved in the KEGG-derived [16] human apoptosis pathway **(hsa04210)**. We chose interleukin 6 (*IL6*) to illustrate the expression coordination of apoptotic genes owing to the significant role played by *IL6* in the PTC development [17]. In addition to the evident independence of the three measures, one may note also the transcriptomic differences between the two histo-pathologically distinct profiled regions from the thyroid.

In this gene selection, FBJ murine osteosarcoma viral oncogene homolog (*FOS*) has the highest average expression level (45.37) in NOR (significantly down-regulated by -2.06x in PTC). Cathepsin H (*CTSH*) had the largest expression (35.23), up-regulated by 6.78x with respect to NOR. *FOS*, cathepsin K *(CTSK)* and inhibitor of kappa light polypeptide gene enhancer in B-cells kinase gamma (*IKBKG*) were among the significantly down-regulated genes. In contrast, H3 interacting domain death agonist (*BID*), cathepsin H (*CTSH*) and diablo, IAP-binding mitochondrial protein (*DIABLO*), were among the up-regulated genes of the selection.

CASP8 and FADD-like apoptosis regulator (*CFLAR*) was the most variably expressed gene in the normal tissue and DNA fragmentation factor, 40kDa, beta polypeptide (caspase-activated DNase) (*DFFB*) the most variably expressed in PTC. Note that most selected genes have larger expression variability in the normal tissue than in the cancer nodule.

Observe also that 20 (40%) of the illustrated apoptotic genes are synergistically expressed with *IL6* in the normal tissue and only 2 (4%) in the PTC, suggesting the decoupling of the programmed cell death from the inflammatory response.

Preprints (www.preprints.org) | NOT PEER-REVIEWED | Posted: 2 August 2020 doi:10.20944/preprints202008.0048.v1

Peer-reviewed version available at Genes 2020, 11, 1030; doi:10.3390/genes11091030

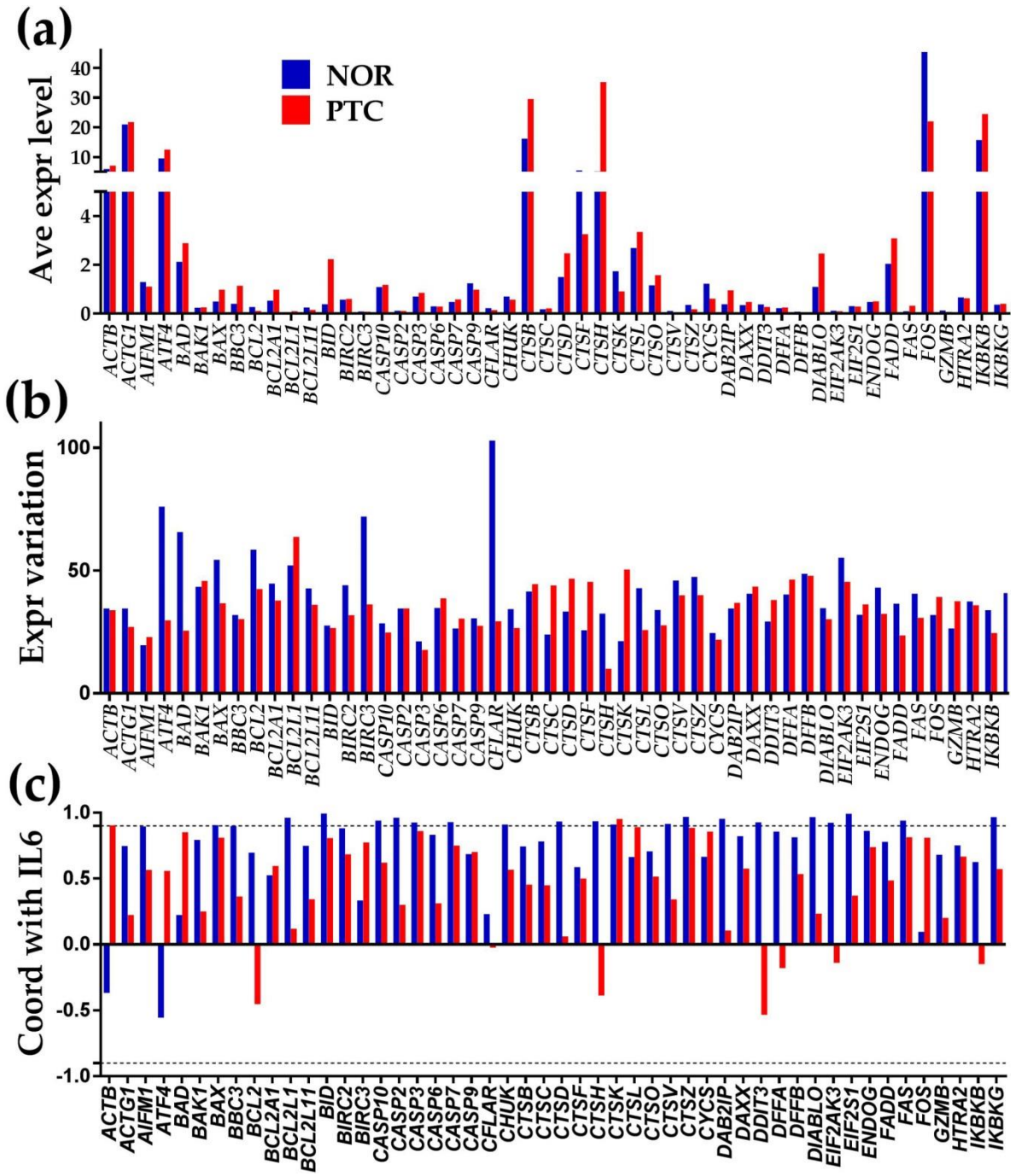

Figure 1 Three independent characteristics of every gene: (a) average expression level, (b) expression variation and (c) expression coordination (here with IL6). The dashed black lines in panel (c) indicate the interval out of which the positive/negative coordination is considered as statistically significant.

3.3. Expression regulation

Figure 2 illustrates the contributions of the first 50 alphabetically ordered oncogenes to the overall regulation in PTC measured by the percentages of the up- and down-regulated genes, expression ratios and weighted individual (gene) regulations. The percentages are restricted to only the significantly regulated genes that are considered as equal contributions. By contrast, both *X* and WIR take into account all (regulated and not regulated) genes and the contributions of these genes are no longer uniform. Moreover, WIR weights the contribution of each gene by its normal expression level, fold-change in cancer and statistical significance of the regulation.

Peer-reviewed version available at Genes 2020, 11, 1030; doi:10.3390/genes11091030

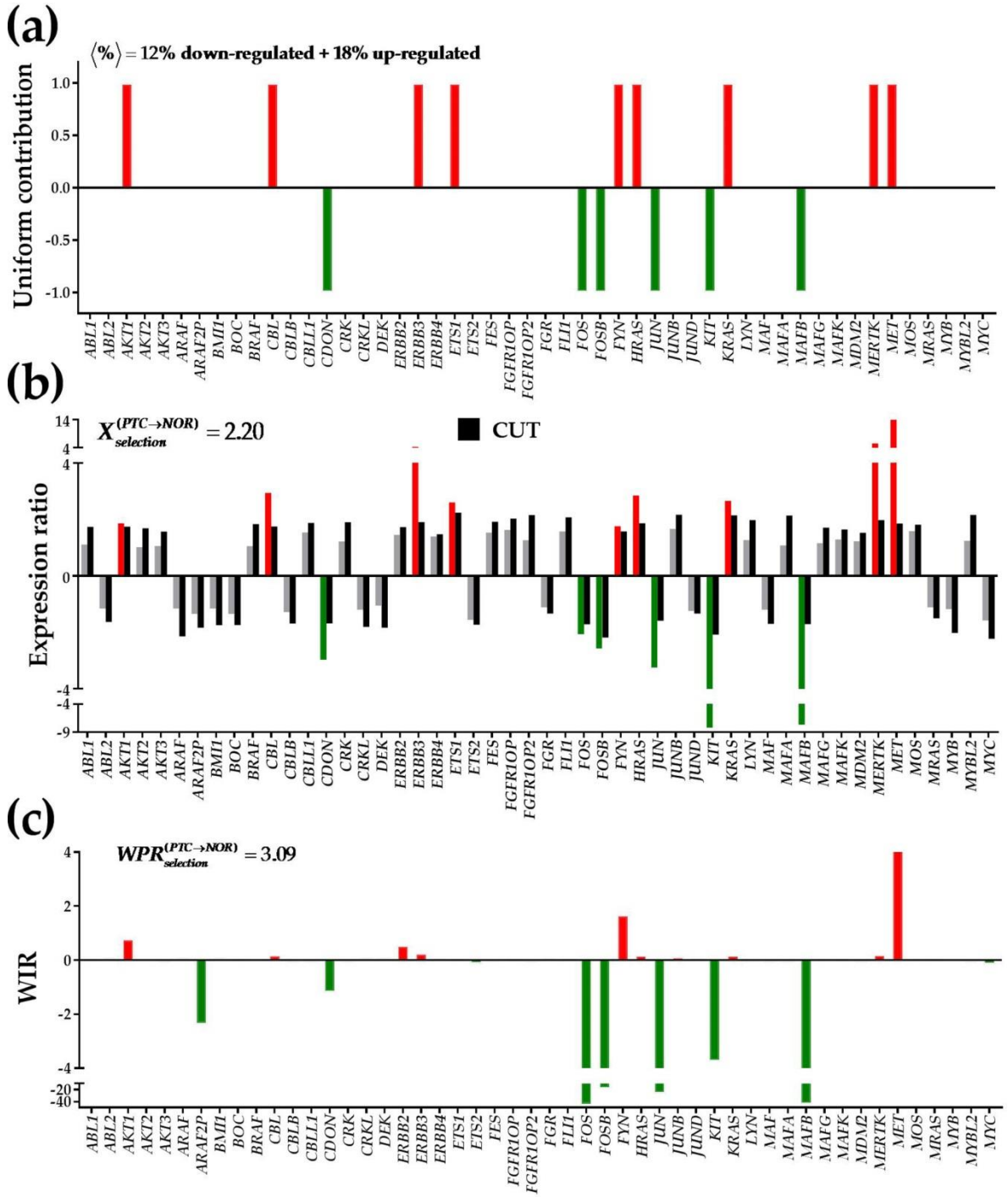

Figure 2 Three ways to consider the contribution of a gene to the pathway regulation: (a) uniform, (b) by expression ratio or (c) as Weighted Individual (gene) Regulation. Red/green/grey **columns** indicate up-/down-/not regulated genes**.** Black columns are the fold-change cut-offs (negative for down-regulation). Regulated genes: v-akt murine thymoma viral oncogene homolog 1 (*AKT1*), Cbl proto-oncogene, E3 ubiquitin protein ligase (*CBL*), cell adhesion associated, oncogene regulated (*CDON*), v-erb-b2 avian erythroblastic leukemia viral oncogene homolog 3 (*ERBB3*), v-ets avian erythroblastosis virus E26 oncogene homolog 1 (*ETS1*), homologs of FBJ murine osteosarcoma viral oncogene (*FOS*/*FOSB*), FYN proto-oncogene, Src family tyrosine kinase (*FYN*), Harvey rat sarcoma viral oncogene homolog (*HRAS*), jun proto-oncogene (*JUN*), Kirsten rat sarcoma viral oncogene homolog (*KRAS*), v-yes-1 Yamaguchi sarcoma viral related oncogene homolog (*LYN*), v-maf avian

musculoaponeurotic fibrosarcoma oncogene homolog B (*MAFB*), c-mer proto-oncogene tyrosine kinase (*MERTK*) and met proto-oncogene (*MET*).

3.4. Regulation of the thyroid hormone synthesis

Figure 3 presents the regulations of the genes involved in the (KEGG-determined) thyroid hormone synthesis (hsa04918). In this pathway, 10.0% of the 50 quantified genes were down-regulated and 8.0% were up-regulated. Compared to the entire transcriptome were the number of up-regulated genes is significantly larger than that of the down-regulated, these percentages indicate that the thyroid function is substantially diminished in PTC.

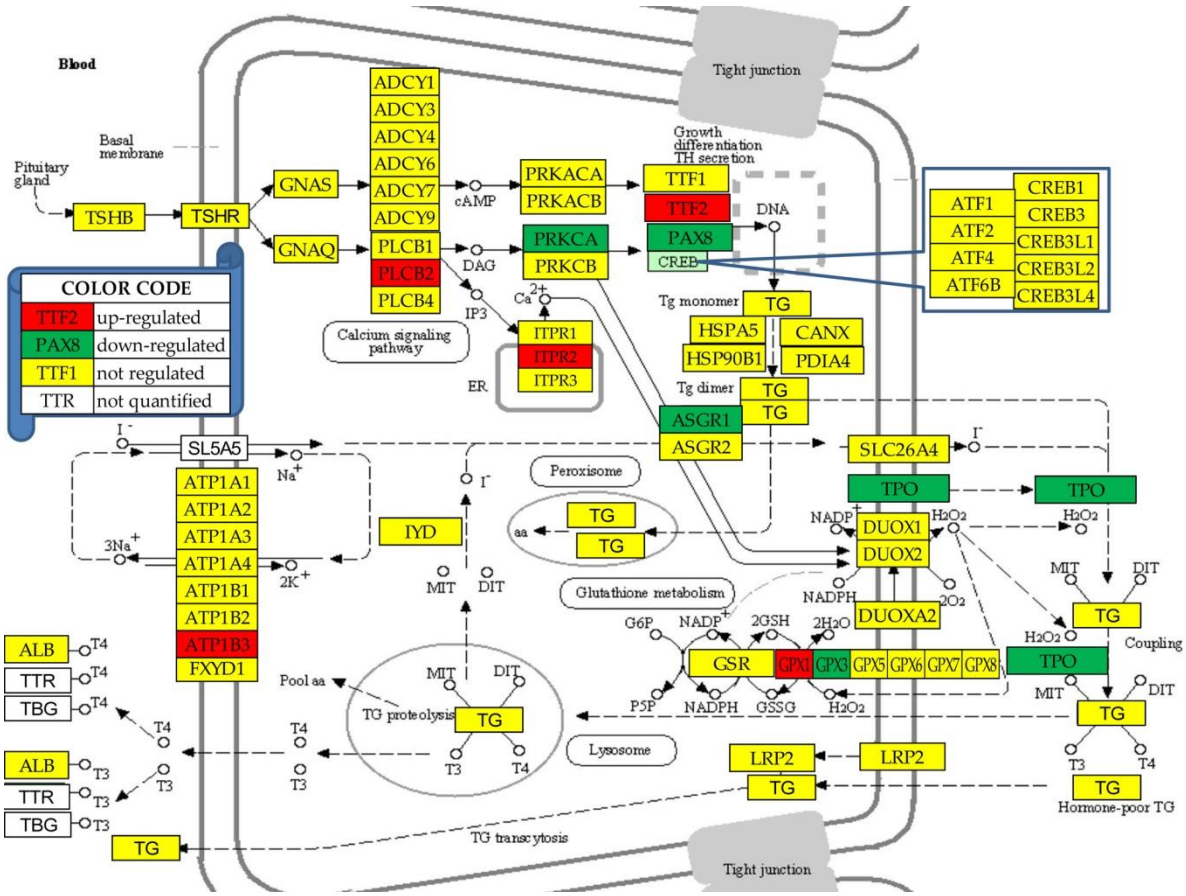

Figure 3 Regulation of thyroid hormone synthesis pathway (modified from hsa04918)**.** Regulated genes: asialoglycoprotein receptor 1 (*ASGR1*), ATPase, Na+/K+ transporting, beta 3 polypeptide (*ATP1B3*), glutathione peroxidases (*GPX1/3*), inositol 1,4,5-trisphosphate receptor, type 2 (*ITPR2*), paired box 8 (*PAX8*), protein kinase C, alpha (*PRKCA*), thyroid peroxidase (*TPO*) and transcription termination factor, RNA polymerase II (*TTF2*).

3.5. Regulation of the cell-cycle pathway

Figure 4 presents the regulation of the genes involved in the (KEGG-determined) cell cycle pathway, where, out of the 93 genes quantified, 3 (3.23%) were down-regulated and 14 (15.05%) were up-regulated. Excepting *PTTG2*, all other regulated genes are located in the DNA replication (S-phase) and the two temporally gaps G1 and G2 separating the S phase from mitosis (M-phase), indicating faster replication but stationary differentiation.

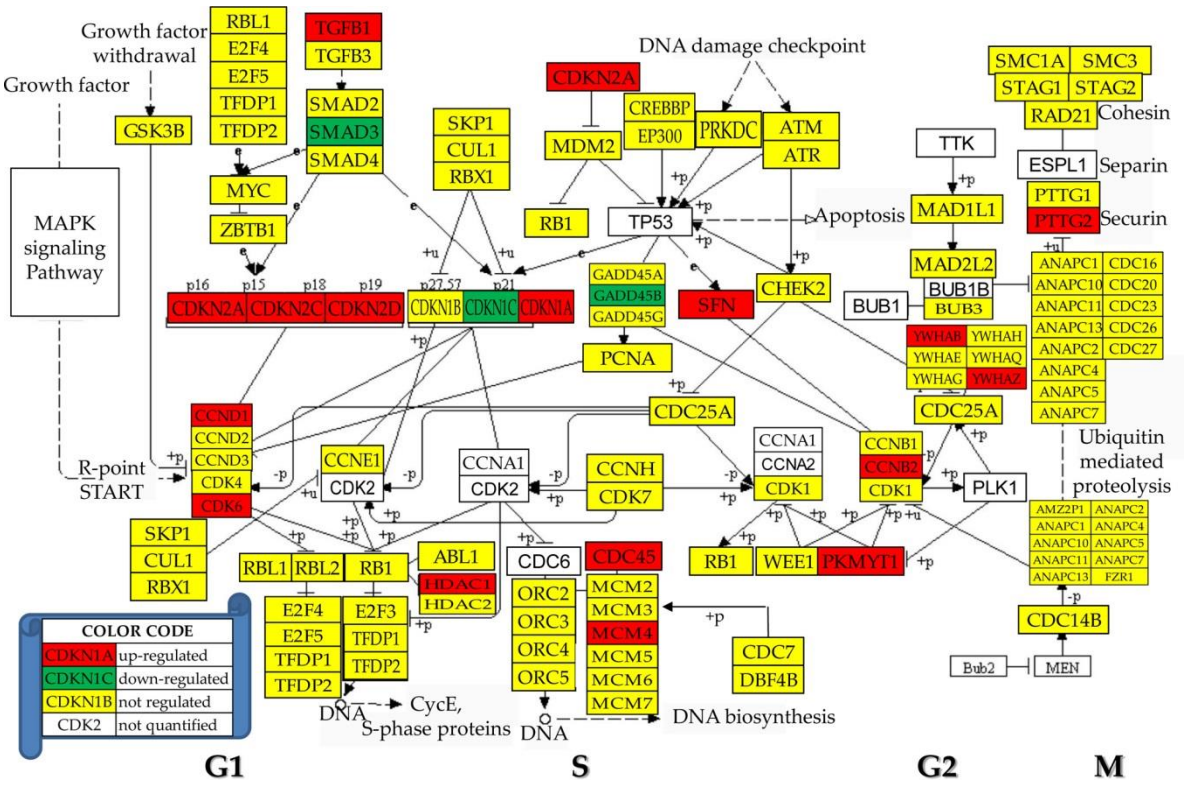

Figure 4 Regulation of the KEGG-determined cell cycle (hsa04110). Regulated genes: cyclin B2 (*CCNB2*), cell division cycle 45 (*CDC45*), cyclin-dependent kinase inhibitors (*CDKN1A/1C/2A/2C/2D*), beta (*GADD45B*), histone deacetylase 1 (*HDAC1*), minichromosome maintenance complex component 4 (*MCM4*), membrane associated tyrosine/threonine 1 (*PKMYT1*), pituitary tumor-transforming 2 (*PTTG2*), stratifin (*SFN*), SMAD family member 3 (*SMAD3*), transforming growth factor, beta 1 (*TGFB1*) and tyrosine 3-monooxygenase/tryptophan 5-monooxygenase activation proteins (*YWHAB/Z*).

3.6. Remodeling of the oxidative phosphorylation pathway

Figure 5 presents the remodeling of the coordination networks among the five complexes of the oxidative phosphorylation in the PTC nodule with respect to NOR tissue. The genes were selected from the KEGG hsa 00190. Note the substantial increase of the synergistically expressed gene pairs in PTC (273) with respect of the NOR (155) and that there is no antagonistically expressed gene pair in PTC while in NOR there are 105. When the coordination inside each complex is added, there are 781 synergistic and 0 antagonistic pairs in PTC versus 458 synergistic and 242 antagonistic pairs in NOR. In addition to the 8 up-regulated vs 3 down-regulated genes within the selection of the 92 oxidative-phosphorylation genes, these results indicate a significant increase in the OP activity.

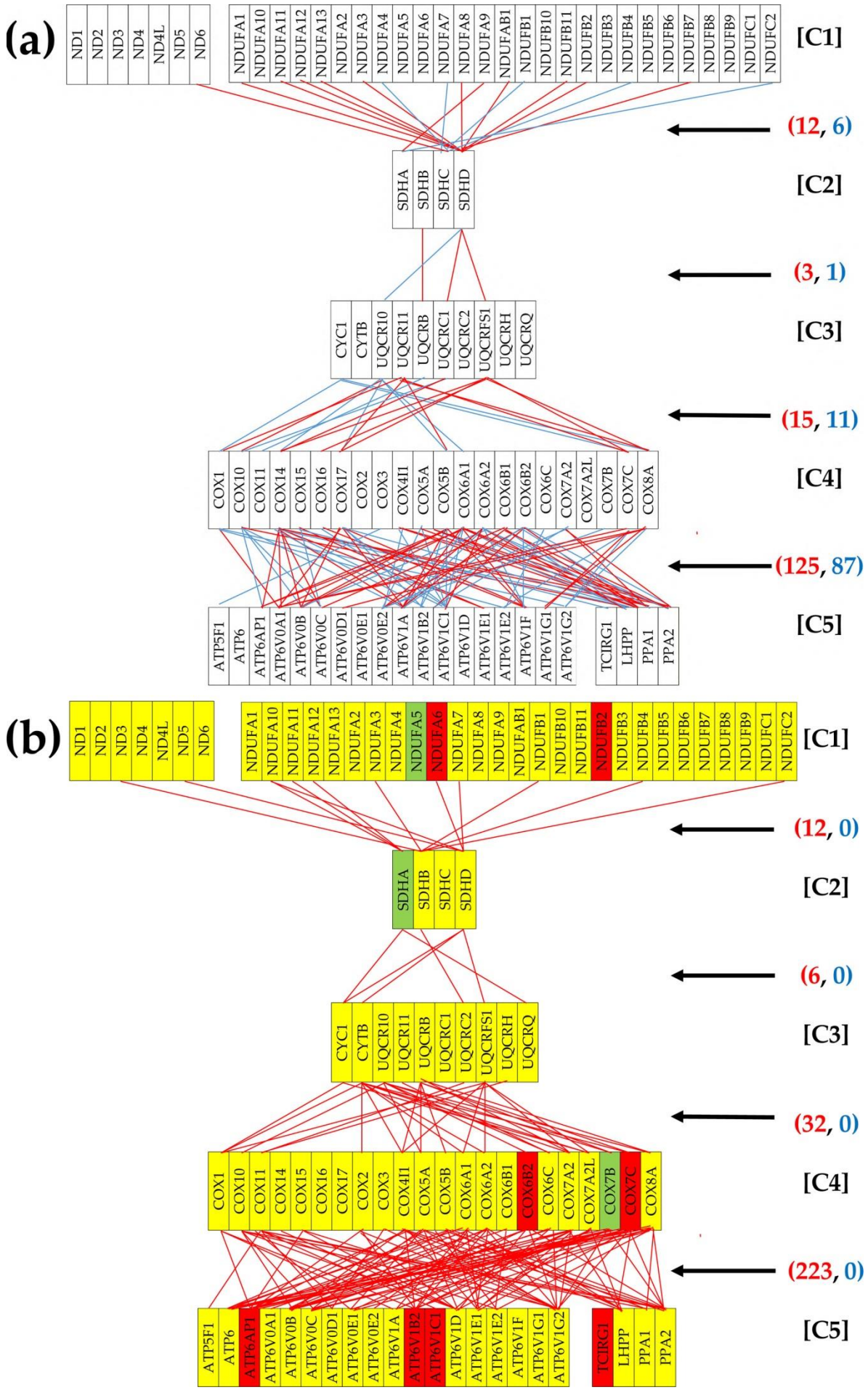

Figure 5: Remodeling of the coordination networks among the five complexes of the oxidative phosphorylation in the PTC nodule with respect to NOR tissue. Regulated genes: ATPase, H+ transporting, lysosomal proteins (*ATP6AP1, ATP6V1B2, ATP6V1C1*), cytochrome c oxidase subunits (*COX6B2, COX7B, COX7C*), NADH dehydrogenase (ubiquinone) 1 alpha/beta subcomplexes (*NDUFA5, NDUFA6, NDUFB2*), succinate dehydrogenase complex, subunit A, flavoprotein (Fp) (*SDHA*) and T-cell, immune regulator 1, ATPase, H+ transporting, lysosomal V0 subunit A3 (TCIRG1)

3.6. Gene hierarchy

Figure 6 presents the GCH scores of the most 12 frequently mutated (as reported in [1]) and the top 12 genes in NOR and PTC. The mutation frequency is also shown (right axis). Note that none of the most frequently mutated genes is among the top 12 genes in either region and that the scores of the top genes in PTC are substantially lower in NOR and vice-versa. These results indicate that none of the most frequently mutated genes (not even *BRAF*, mutated in 20.56% of the 1,440 cases) has a competitive GCH to be a good candidate for the PTC gene therapy (GCH of *BRAF* in PTC is 11.79). However, *SPINT2*, the PTC's GMR ($GCH_{SPINT2}^{(PTC)}$ = 54.97), appears to be the most legitimate target for this case. Moreover, we speculate that while significant alteration of the expression of *SPINT2* would have lethal impact on the cancer cells, owing the very low GCH in NOR ($GCH_{SPINT2}^{(NOR)}$ = 1.93) it might have very little consequences on the normal cells.

For comparison, we added also the GCH scores of the top genes in the standard thyroid cancer cell lines: BCPAP (papillary) and 8505C (anaplastic). As additional reference, Figure S1 in the Appendix A shows the GCH scores of most of the genes from FoundationOne®CDx used by Foundation Medicine [13] for genomic testing of solid tumors, including "Non-Small Cell Lung (NSCLC), Colorectal, Breast, Ovarian, and Melanoma. The list contains genes with full coding exonic regions for the detection of substitutions, insertion-deletions (indels), and copy-number alterations (CNAs). It also contains genes with select intronic regions for the detection of gene rearrangements, one gene with a promoter region (*TERT* = telomerase reverse transcriptase) and one non-coding RNA gene (*TERC*). These genes might be useful for diagnostic purposes. However, with their GCH score far below the GMR's and with not enough difference between PTC and NOR, they should have little therapeutic value for this particular case. Substantially lower than the PTC GMR were the biomarkers, oncogenes, apoptosis genes and the ncRNAs determined in the same specimens and presented in Figure 2, Ref [8].

Preprints (www.preprints.org) | NOT PEER-REVIEWED | Posted: 2 August 2020 doi:10.20944/preprints202008.0048.v1

Peer-reviewed version available at Genes 2020, 11, 1030; doi:10.3390/genes11091030

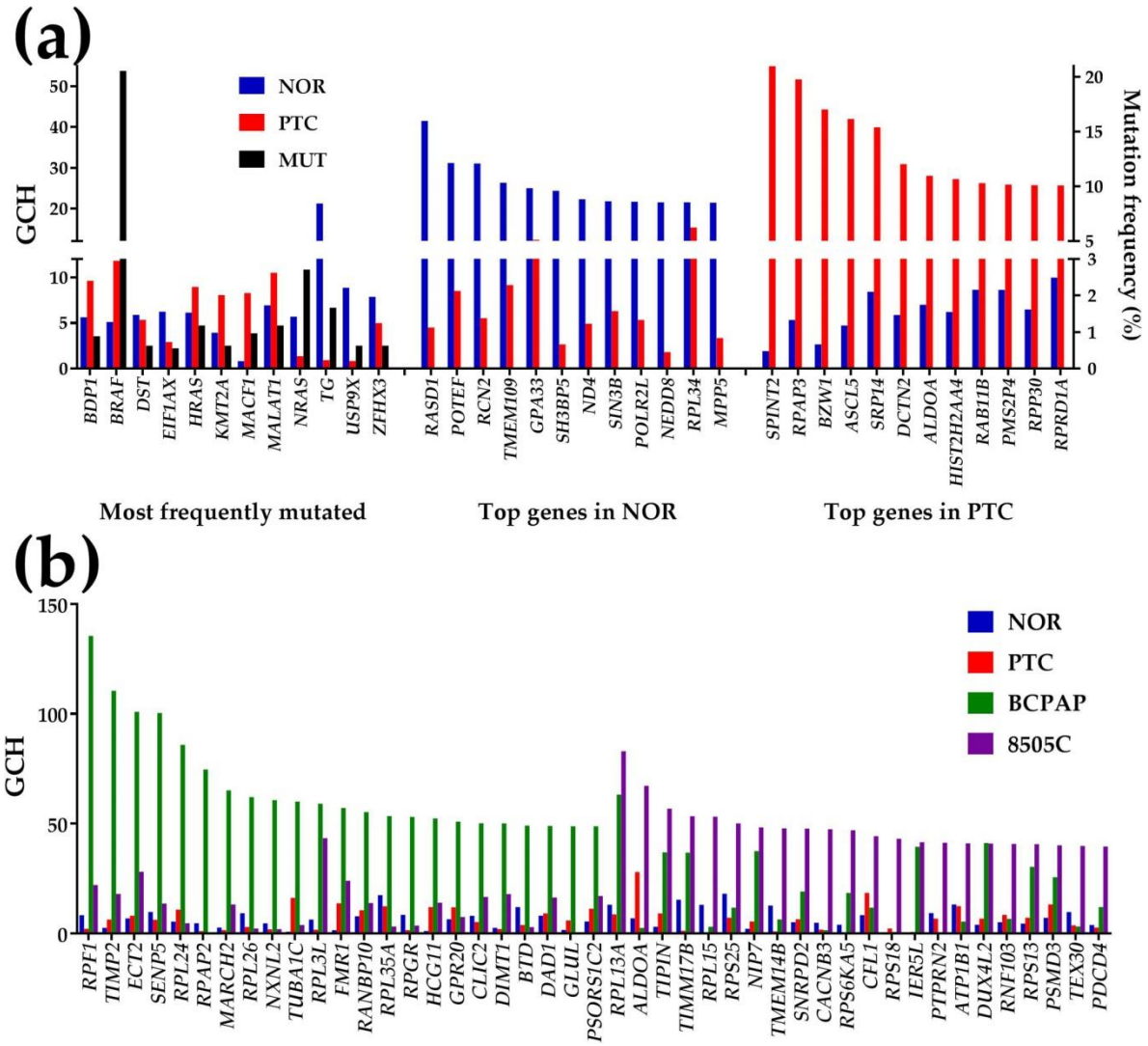

Figure 6 Gene Commanding Height (GCH). (a) GCH and mutation frequency of 12 reported most frequently mutated genes and the top 12 genes in the normal tissue (NOR) and the papillary nodule (PTC). (b) GCH of the top 23 genes in the papillary (BCPAP) and anaplastic (8505C) thyroid cancer cell line. Mutated genes: *BDP1* (B double prime 1, subunit of RNA polymerase III transcription initiation factor IIIB), *BRAF* (B-Raf proto-oncogene, serine/threonine kinase), *DST* (dystonin), *EIF1AX* (eukaryotic translation initiation factor 1A, X-linked), *HRAS* (Harvey rat sarcoma viral oncogene homolog), *KMT2A* (lysine (K)-specific methyltransferase 2A), *MACR1* (microtubule-actin crosslinking factor 1), *MALAT1* (metastasis associated lung adenocarcinoma transcript 1 (non-protein coding)), *NRAS* (neuroblastoma RAS viral (v-ras) oncogene homolog), *TG* (thyroglobulin), *USP9X*(ubiquitin specific peptidase 9, X-linked), *ZFHX3* (zinc finger homeobox 3). **Top 3 genes in NOR:** RAS, dexamethasone-induced 1 (*RASD1*), POTE ankyrin domain family, member F (*POTEF*), reticulocalbin 2, EF-hand calcium binding domain (*RCN2*). **Top 3 genes in PTC:** serine peptidase inhibitor, Kunitz type, 2 (*SPINT2*), RNA polymerase II associated protein 3 (*RPAP3*), basic leucine zipper and W2 domains 1 (*BZW1*).

3.7. The Gene Master Regulator at play

Our study identified *SPINT2* as the GMR of this patient's malignancy. A legitimate question is how a not regulated gene in the cancer nodule with respect to the surrounding normal tissue can be the PTC "Commander-in Chief" so that its significant regulation would selectively kill the cancer cells? In order to determine what deleterious effects the regulation of *SPINT2* may have, we analyzed its expression coordination of *SPINT2* with 112 apoptosis genes in the two regions (Fig. 7).

Preprints (www.preprints.org) | NOT PEER-REVIEWED | Posted: 2 August 2020 doi:10.20944/preprints202008.0048.v1

Peer-reviewed version available at Genes 2020, 11, 1030; doi:10.3390/genes11091030

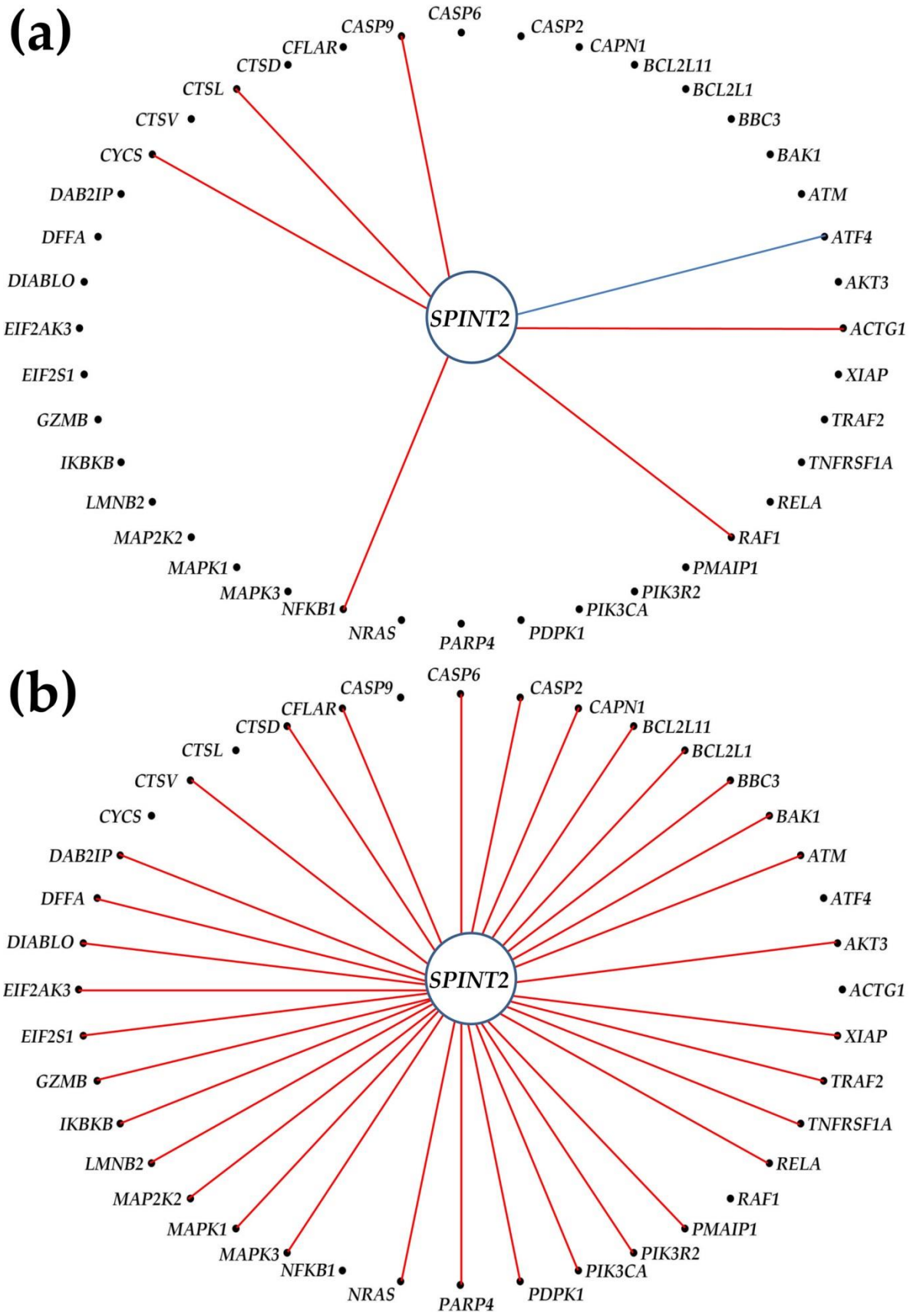

Figure 7 Expression coordination of *SPINT2*, the PTC-GMR with apoptosis genes in (a) NOR and (b) PTC. A red/blue line indicates that the linked genes are synergistically/antagonistically expressed. Only the significant expression coordination links in at least one region were presented.

In PTC (20 significantly up-regulated and 7 down-regulated), we found *SPINT2* as significantly synergistically expressed with 35 genes, but no significant antagonism or independence. This a substantial increase from the 6 synergistically, 1 antagonistically (*ATF4* = activating transcription factor 4) and 4 independently (*BCL2*, *IKBKB*, *TUBA1C*, *TUBA3D*) expressed apoptotic partners of *SPINT2* in NOR. Interestingly, none of the significant coordinations in NOR (with: *ACTG1*, *ATF4*, *CASP9*, *CTSL*, *CYCS*, *NFKB1*) were maintained in PTC.

What effect up-regulation of an otherwise stably expressed but not regulated gene in PTC may have on cancer cells? We speculate that, owing to the substantial expression synergistic coordination with apoptosis genes, the experimental up-regulation of *SPINT2* would up-regulate many of these genes, forcing the commanded cells (PTC) to enter programmed death.

There was no way to validate this hypothesis on the patient from whom we have profiled the thyroid tumor samples. However, we tested the general hypothesis that expression coordination with one gene predicts expression regulation when the expression of that gene is experimentally manipulated. For this purpose, we reanalyzed the transcriptomes of the thyroid cancer cell lines BCPAP and 8505C cells before and after stably lentiviral transfection with *DDX19B* [7]. Figure 8ab plots the correlation coefficient with *DDX19B* in the untreated cells against the fold-changes (negative for down-regulation) of the genes in the transfected cells. They clearly show that expression coordination predicts with reasonable accuracy (> 86%) the expression regulation. Thus, most genes synergistically expressed with *DDX19B* in untransfected cells were up-regulated in the transfected ones and most genes antagonistically expressed with *DDX19B* in untransfected cells were down-regulated in the transfected ones. Based on this validation, Figure 8c illustrates the predicted regulations of apoptosis genes if the expression level of *SPINT2* in PTC is significantly increased.

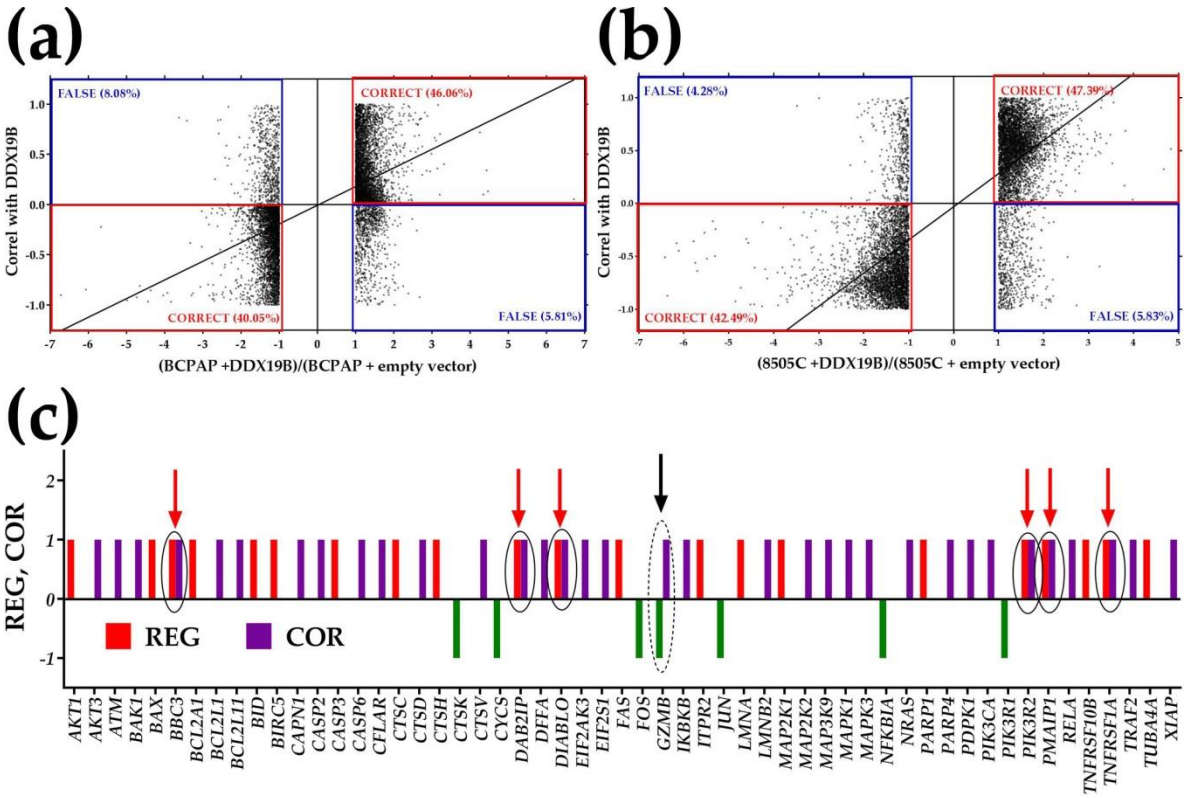

Figure 8 Prediction of the ripple effects of gene experimental regulation. (a) Expression coordination with *DDX19B* in untreated BCAP cells predicts (40.05 + 46.06 =) **86.11% of the expression regulations in BCAP cells stably transfected with *DDX19B*; (b) Expression coordination with *DDX19B* in untreated 8505C cells predicts** (42.49 + 47.39 =) **89.88% of the regulations in 8505C cells stably transfected with *DDX19B*; (c) Predicted regulation (1 for up-regulation and -1 for down-regulation) of apoptotic genes in PTC following experimental**

overexpression of *SPINT2*. REG = significant (1 = up-regulation, -1 = down-) regulation. COR = significant expression synergism. Only the regulated genes in the untreated PTC and those expected to be regulated in treated PTC are represented. Red arrows indicate combined effect in treated tumor of regulation and expression synergism in untreated PTC. The black arrow indicates the down-regulation in untreated PTC expected to be compensated by the overexpression of *SPINT2*.

In Fig. 8c we used the uniform contribution of the significantly altered genes to the percentages of (up-/down-) regulated genes. Note that from 20 up-regulated and 6 down-regulated genes in untreated PTC, overexpression of *SPINT2* may result in 48 up-regulated and 6 down-regulated genes. Expression of 6 (*BBC3, DAB2IP, DIABLO, PIK3R2, PMAIP1, TNFRSF1A*) already regulated genes in PTC may be further increased by treatment, while the down-regulation of *GZMB* in untreated is recovered in treated cells.

4. Discussion

The analyses presented in this report are consistent with the genomic fabric paradigm [18] which considers the transcriptome as a multi-dimensional object: 3 independent features for each gene x N expressed genes - the dynamic set of expression correlations among the genes. The traditional transcriptomic analyses are limited to only the expression level of individual genes and comparisons of the expression levels of distinct genes in the same condition or of the same gene in different conditions. Our procedure considerably enlarges the transcriptomic information by considering instead of one three independent features for each gene and all possible combinations of these features and their comparisons among the genes and across the conditions.

Although high levels of *EEF1A1* were reported in renal cell carcinoma [19], we found this gene with the highest expression in NOR and with one of the highest levels in PTC (68.47), albeit not significantly down-regulated. High expression of *NPC2* and its significant elevation in PTC were also detected in meta-analyses of public PTC transcriptomes [20]. Overexpression of *CHI3L1*, the most up-regulated gene in the analyzed PTC, was reported as associated with metastatic PTC [21] and its recurrence [22]. Significantly decreased expression of *TFF3*, the most down-regulated gene in our study, was also reported in several other studies (e.g.: [23]).

In addition to illustrating the independence of the three features, Fig. 1 provides likewise some interesting findings and confirmations of results reported by other authors. For instance, the high expression of *CTSH* in PTC (up-regulated by 6.78x with respect to NOR) was related to the tumor progression and migration of cancer cells [24].

The median REV decreases statistically significant (p-val = 7.79×10^{-5}) from 39.75 in NOR to 38.69 in PTC. According to the Second Law of Thermodynamics, the significantly larger overall expression variability in NOR than in PTC indicates not only relaxed control by the homeostatic mechanisms (average REC_{NOR} = 0.084, average REC_{PTC} = 0.113) but also that NOR is closer to the thermodynamic (here physiological) equilibrium. Supporting this assertion is the reduction of the median REV observed by us in all other gene expression studies on animal models of human diseases (e.g.: [25-27]) and in tissues of animals subjected to various stresses (e.g.:[28-31] or to genetic manipulations (e.g. [32,33]). The high expression variability of *CFLAR* (a key anti-apoptosis regulator [34]) in NOR (REV = 102.93) may explain the adaptability of the apoptosis pathway to a large spectrum of environmental conditions. *CFLAR* REV dramatic reduction in PTC (REV =29.41) shows the need of a tighter control of resisting apoptosis in cancer. Moreover, its reduction of expression level (in PTC by -1.64x) was associated with delayed apoptosis [34].

The observed down-regulation of *FOS* in PTC (Fig. 2) confirms findings of some groups [35,36] but contradicts its frequent (but not 100%) up-regulation reported by other group in 40 patients with thyroid cancer and 20 with benign thyroid diseases [37]. Let us analyze what measure of regulation is the most accurate and take the examples of *FOS* and *KIT* (another gene down-regulated in thyroid cancer [38]). Although both genes account as units for the percentage of the down-regulated genes, they contribute with -2.06x and -8.15x as expression ratios and with -46.28 and -3.76 as WIRs. Since WIR is a more comprehensive measure, we speculate that *FOS* regulation is the most important

factor in the alteration of this group of genes. Indeed, FOS protein is an important player in cell proliferation, differentiation, transformation and apoptotic cell death.

Among the significantly regulated genes from the KEGG-derived THS pathway (map hsa04918, Fig. 3) only *PAX8* (-1.94x) was previously related to the thyroid cancer, albeit to the follicular form. Moreover, we found that peroxisome proliferator-activated receptor gamma (*PPARG*) whose fusion with *PAX8* is considered an important trigger of the FTC [39], was likewise significantly down-regulated (-4.99x). Interestingly, in Fig. 3, the two glutathione peroxidases: *GPX1* (1.60x) and *GPX3* (-1.84x) were oppositely regulated. Since down-regulation of *GPX1* was reported to augmenting the pro-inflammatory cytokine-induced redox signaling and endothelial cell activation [40], one may assume that up-regulation of *GPX1* will do the opposite, i.e. diminish the pro-inflammatory cytokine-induced redox signaling. As such, the PTC cells will become more resistant to the inflammatory response.

According to the KEGG map hsa04110, some of the regulated cell-cycle genes (Fig. 4) were associated with a wide diversity of cancers. Thus, up-regulation of *CDKN1A* was associated with cervical [41] and down-regulation of *CDKN1C* with gastric [42] cancers. As stated in [3], up-regulation/mutation of *CDKN2A* were detected in almost all forms of cancer: neoplasms (squamous cell, ductal, lobular, cystic, mucinous, serous, mesothelial, lipomathous, myomathous, tymic epithelial, complex, mixed), adenomas, adenocarcionmas, gliomas, nevi and melanomas, transitional cell papillomas and carcinomas, mature b-cell lymphomas, soft tissue tumors and sarcomas. *CDKN2B* was associated with malignant pleural mesothelioma, osteosarcoma and meningioma. However, none of these genes has been associated with thyroid cancer yet. Unfortunately, the most cancer-related gene, *TP53*, was not quantified in this experiment.

As illustrated in Figure 5 for interlinks between the five complexes of the oxidative phosphorylation, cancer remodels the gene networks, profoundly perturbing the mitochondrial function [43]. Among others, 10 synergistically expressed gene pairs in NOR are switched into antagonistically expressed pairs in PTC: *NDUFA10-SDHD, CYC1-COX1, COX10-ATP6V0B, COX10-ATP6V0C, COX5B-LHPP, COX6A1-ATV1B2, COX6A1-LHPP, COX6A2-ATP6V0B, COX6A2-ATP6V1A, COX7C-ATP6V1G2*. These switches, the cancellation of all significant antagonisms and the added synergisms increase the expression synchrony of the pathway genes [12] and remove the controlling bottlenecks. In a synergistic pair, up-regulation of one gene triggers up-regulation of the other. Although in this experiment we did not detect significant altered expressions of *NDUFA10* and *SDHD*, their significant synergism in PTC may explain why they are both up-regulated in oral cancer [44].

Given the never repeatable set of risk factors, each patient is unique and therefore its gene hierarchy is unique. Although, the chance to find the same GMR in two persons is about 1/20,000 and that of the first two genes is 1/400 mil, from the first 3 genes up the number of possibilities (7.9988×10^{12}) exceeds by far the Earth human population. Therefore, the first three genes are enough to uniquely represent the cancer of each person at a given time. In our studied PTC, the top 3 genes were: *SPINT2*, *RPAP3* and *BZW,1* none of them being significantly regulated with respect to NOR.

SPINT2, the identified GMR of the profiled PTC (Fig. 6), was previously reported by several groups as involved in the development and progression of wide diversity forms of cancer [45]. Among others, *SPINT2* was associated with metastatic osteosarcoma [46], ovarian cancer [47], glioma/glioblastoma [48, 49], prostate [50] and non-small lung [51] cancers, leukemia [52] and cervical carcinoma [53]. *RPAP3*, essential for assembling chaperone complexes [54], was linked to hypoxia adapted cancer cells [55] and *BZW,1* was associated with ovarian [56], lung [57] and salivary gland [58] cancers. However, we found no mention in the literature about the role of these first three genes in any form of thyroid cancer.

In Figures 7 and 8 we tested whether expression synergism with apoptosis genes may be one of the mechanisms by which manipulation of *SPINT2* expression is lethal to the PTC cells but not to the NOR cells. First, we determined the significant coordination apoptosis partners of *SPINT2* in both NOR and PTC and found a substantial increase of the expression synergism in PTC. Then, we showed the remarkable predictive value of the expression coordination in untreated cells for the

regulation in treated ones. Figures 8ab confirm our previous findings that expression correlation with one gene predicts what genes are regulated when the expression of that gene is manipulated. For instance in [59], we have shown that most genes synergistically/antagonistically expressed with *Gja* (encoding the gap junction protein Cx43) in brain and hearts of wildtype mice are down-/up-regulated in brain and hearts of Cx43KO mice. Therefore, as illustrated in Fig. 8c, we expect that, owing to the synergism, overexpression of *SPINT2* will force the PTC cells into programmed death by up-regulating the apoptosis genes.

5. Conclusions

This study provides additional reasons in favor of a personalized and time-sensitive cancer gene therapy based on the manipulation of the gene master regulators.

Supplementary Materials: The following are available online at www.mdpi.com/xxx/s1, Figure S1: GCH scores of the genes included in FoundationOne®CDx assay.

Funding: This research was possible owing to the Texas A&M University System Chancellor's Research Initiative (CRI) funding for the Center for Computational Systems Biology at the Prairie View A&M University.

Conflicts of Interest: The author declares no conflict of interest.

Appendix A

Preprints (www.preprints.org) | NOT PEER-REVIEWED | Posted: 2 August 2020 doi:10.20944/preprints202008.0048.v1

Peer-reviewed version available at Genes 2020, 11, 1030; doi:10.3390/genes11091030

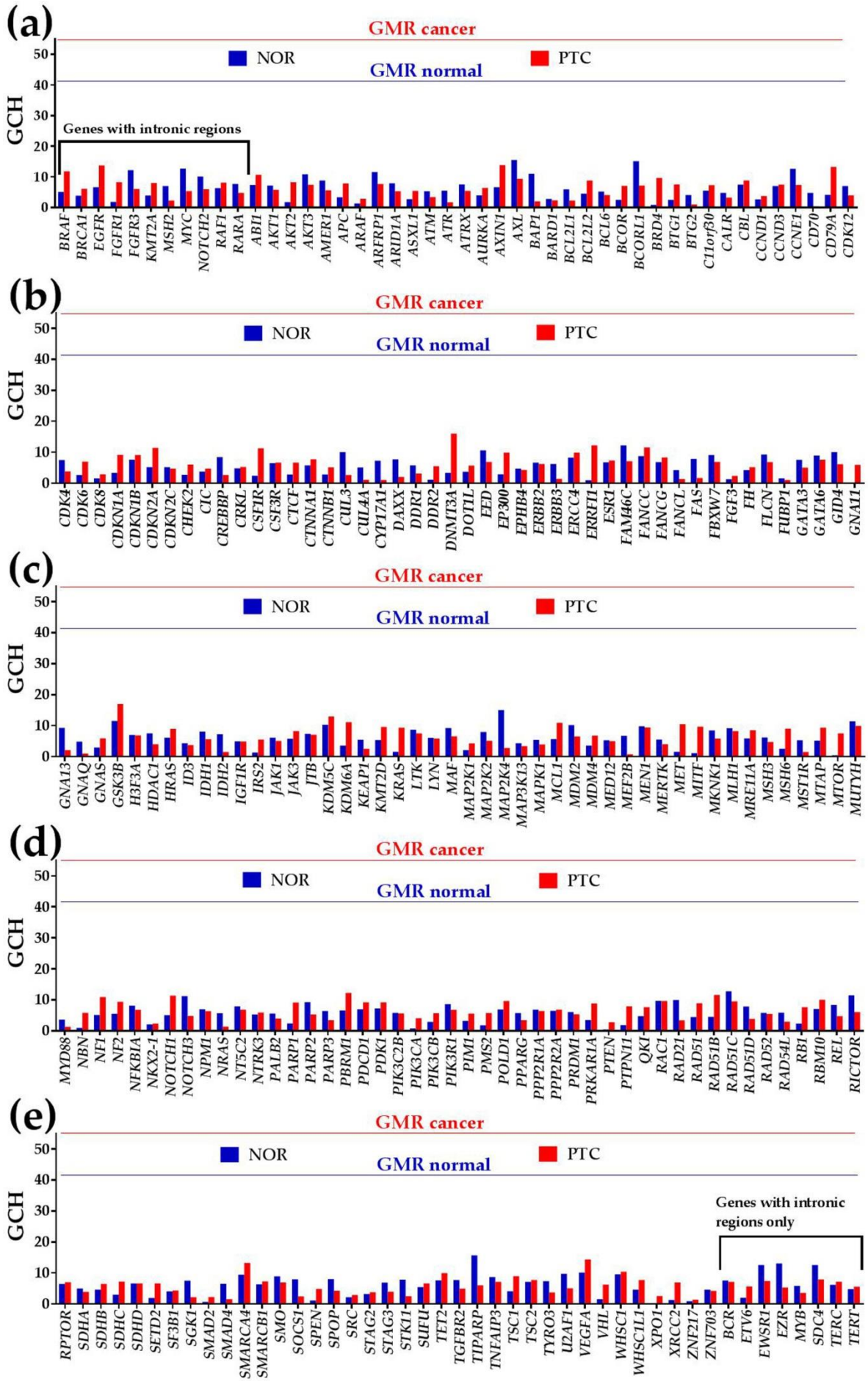

Figure S1 GCH scores of the genes included in FoundationOne®CDx assay. The assay explores genes with full coding exonic regions for the detection of substitutions, insertion-deletions (indels), and copy-number alterations (CNAs), genes with select intronic regions for the detection of gene rearrangements, one gene with a promoter region and one non-coding RNA gene. Several genes (*BRAF, BRCA1, EGFR, FGFR1/3, KMT2A, MSH2, MYC. NOTCH2, RAF1, RARA*) have both exonic and intronic regions used for detection.

References

1. https://www.cancer.org/cancer/thyroid-cancer, accessed 07/26/2020
2. https://www.thyroid.org/thyroid-cancer/, accessed 07/26/2020
3. https://portal.gdc.cancer.gov, accessed 07/26/2020
4. Alexander, E. K.; Kennedy, G. C.; Baloch, Z. W.; Cibas, E. S.; Chudova, D.; Diggans, J.; Friedman, L.; Kloos, R. T.; LiVolsi, V. A.; Mandel, S. J. et al. Preoperative diagnosis of benign thyroid nodules with indeterminate cytology. *N Engl J Med* **2012**, 367(8), 705–715. Doi: 10.1056/NEJMoa1203208
5. Abdullah, M.I.; Junit, S.M.; Ng, K.L.; Jayapalan, J.J.; Karikalan, B.; Hashim, O.H. Papillary Thyroid Cancer: Genetic Alterations and Molecular Biomrker Investigations. *Int J Med Sci* **2019** 16(3):450-460. doi: 10.7150/ijms.29935.
6. https://www.foundationmedicine.com/genomic-testing, accessed 07/12/2020
7. Iacobas, D.A.; Tuli, N.; Iacobas, S.; Rasamny, J.K.; Moscatello, A.; Geliebter, J.; et al. Gene master regulators of papillary and anaplastic thyroid cancer phenotypes. *Oncotarget* **2018**, 9(2), 2410-2424. doi: 10.18632/oncotarget.23417. PMID: 29416781.
8. Iacobas, S.; Ede, N.; Iacobas, D.A. The Gene Master Regulators (GMR) Approach Provides Legitimate Targets for Personalized, Time-Sensitive Cancer Gene Therapy. *Genes* **2019**, 10(8), 560. doi: 10.3390/genes10080560. PMID: 31349573.
9. Iacobas, D,A.; Iacobas, S. Towards a Personalized Cancer Gene Therapy: A Case of Clear Cell Renal Cell Carcinoma. *Cancer & Oncol Res* **2017**, 5(3): 45-52. DOI:10.13189/cor.2017.050301
10. https://www.ncbi.nlm.nih.gov/geo, accessed 07/26/2020
11. Iacobas, D.A.; Iacobas, S.; Stout, R.; Spray, D.C. Cellular environment remodels the genomic fabrics of functional pathways in astrocytes. *Genes (Basel)* **2020**, 11(5), 520; doi: 10.3390/genes11050520 .
12. Iacobas, D.A.; Iacobas, S.; Lee, P.R.; Cohen, J.E.; Fields, R.D. Coordinated Activity of Transcriptional Networks Responding to the Pattern of Action Potential Firing in Neurons. *Genes (Basel)* **2019**, 10(10), 754. PMID: 31561430, Doi: 10.3390/genes10100754.
13. Mathew, R.; Huang, J.; Iacobas, S.; Iacobas, D.A. Pulmonary Hypertension Remodels the Genomic Fabrics of Major Functional Pathways. *Genes* **2020**, *11*, 126, doi:10.3390/genes11020126.
14. Iacobas, D.A.; Iacobas, S.; Tanowitz, H.B.; deCarvalho, A.C.; Spray, D.C. Functional genomic fabrics are remodeled in a mouse model of Chagasic cardiomyopathy and restored following cell therapy. *Microbes Infect* **2018**, 20(3), 185-195. doi: 10.1016/j.micinf.2017.11.003.
15. Kanehisa, M.; Furumichi, M.; Tanabe, M.; Sato, Y. Morishima, K. KEGG: new perspectives on genomes, pathways, diseases and drugs. *Nucleic Acids Res* **2017**, 45, D353-D361. DOI: 10.1093/nar/gkw1092
16. http://www.genome.jp/kegg/, accessed 06/21/2020
17. Kobawala, T.P.; Trivedi, T.I.; Gajjar, K.K.; Patel, D.H.; Patel, G.H., Ghosh, N.R. Significance of Interleukin-6 in Papillary Thyroid Carcinoma. *J Thyroid Res* **2016**, 6178921. doi.org/10.1155/2016/6178921.
18. Iacobas, D.A. The Genomic Fabric Perspective on the Transcriptome between Universal Quantifiers and Personalized Genomic Medicine. *Biological Theory* **2016**, 11(3): 123-137. DOI 10.1007/s13752-016-0245-3.
19. Bao, Y.; Zhao, T.L.; Zhang, Z.Q. Liang, X.L.; Wang, Z.X.; Xiong, Y.; Lu, X.; Wang, L.H. High eukaryotic translation elongation factor 1 alpha 1 expression promotes proliferation and predicts poor prognosis in clear cell renal cell carcinoma. *Neoplasma*. **2020**; 67(1):78-84. doi: 10.4149/neo_2019_190224N158. PMID: 31777262.
20. Wu, C.C.; Lin, J.D.; Chen, J.T.; Chang, C.M.; Weng, H.F.; Hsueh, C.; Chien, H.P.; Yu, J.S. Integrated analysis of fine-needle-aspiration cystic fluid proteome, cancer cell secretome, and public transcriptome datasets for papillary thyroid cancer biomarker discovery. *Oncotarget*. **2018**; 9(15):12079-12100. doi: 10.18632/oncotarget.23951. PMID: 29552294; PMCID: PMC5844730.
21. Luo, D.; Chen, H.; Lu, P.; Li, X.; Long, M.; Peng, X.; Huang, M.; Huang, K.; Lin, S.; Tan, L. et al. CHI3L1 overexpression is associated with metastasis and is an indicator of poor prognosis in papillary thyroid carcinoma. *Cancer Biomark*. **2017**; 18(3):273-284. doi: 10.3233/CBM-160255. PMID: 28009325.
22. Cheng, S.P.; Lee, J.J.; Chang, Y.C.; Lin, C.H.; Li, Y.S.; Liu, C.L. Overexpression of chitinase-3-like protein 1 is associated with structural recurrence in patients with differentiated thyroid cancer. *J Pathol*. **2020**. doi: 10.1002/path.5503. Epub ahead of print. PMID: 32613636.
23. Oczko-Wojciechowska, M.; Pfeifer, A.; Jarzab, M.; Swierniak, M.; Rusinek, D.; Tyszkiewicz, T.; Kowalska, M.; Chmielik, E.; Zembala-Nozynska, E.; Czarniecka, A. et al. Impact of the Tumor Microenvironment on

the Gene Expression Profile in Papillary Thyroid Cancer. *Pathobiology*. **2020**; 87(2):143-154. doi: 10.1159/000507223. PMID: 32320975.

24. Jevnikar, Z.; Rojnik, M.; Jamnik, P.; Doljak, B.; Fonovic, U.P.; Kos J. Cathepsin H mediates the processing of talin and regulates migration of prostate cancer cells. *J Biol Chem*. **2013,** 288(4):2201-9. doi: 10.1074/jbc.M112.436394. PMID: 23204516; PMCID: PMC3554893.
25. Iacobas, D.A. The Genomic Fabric Perspective on the Transcriptome between Universal Quantifiers and Personalized Genomic Medicine. *Biol. Theory* **2016**, *11*, 123–137, doi:10.1007/s13752-016-0245-3.
26. Iacobas, D.A.; Iacobas, S.; Werner, P.; Scemes, E.; Spray, D.C. Alteration of transcriptomic networks in adoptive-transfer experimental autoimmune encephalomyelitis. *Front. Integr. Neurosci.* **2007**, *1*, doi:10.3389/neuro.07/010.2007.
27. Iacobas, D.A.; Iacobas, S. Towards a Personalized Cancer Gene Therapy: A Case of Clear Cell Renal Cell Carcinoma. *Cancer Oncol. Res.* **2017**, *5*, 45–52, doi:10.13189/cor.2017.050301.
28. Frigeri, A.; Iacobas, D.A.; Iacobas, S.; Nicchia, G.P.; Desaphy, J.-F.; Camerino, D.C.; Svelto, M.; Spray, D.C. Effect of microagravity on brain gene expression in mice. *Exp. Brain Res.* **2008**, *191*, 289–300, doi:10.1007/s00221-008-1523-5.
29. Iacobas, D.A.; Fan, C.; Iacobas, S.; Spray, D.C.; Haddad, G.G. Transcriptomic changes in developing kidney exposed to chronic hypoxia. *Biochem. Biophys. Res. Commun.* **2006**, *349*, 329–338, doi:10.1016/j.bbrc.2006.08.056.
30. Iacobas, D.A.; Fan, C.; Iacobas, S.; Haddad, G.G. Integrated transcriptomic response to cardiac chronic hypoxia: Translation regulators and response to stress in cell survival. *Funct. Integr. Genom.* **2008**, *8*, 265–275, doi:10.1007/s10142-008-0082-y.
31. Iacobas, D.A.; Iacobas, S.; Haddad, G.G. Heart rhythm genomic fabric in hypoxia. *Biochem. Biophys. Res. Commun.* **2010**, *391*, 1769–1774, doi:10.1016/j.bbrc.2009.12.151.
32. Iacobas, D.A.; Urban, M.; Iacobas, S.; Scemes, E.; Spray, D.C. Array analysis of gene expression in connexin43 null astrocytes. *Physiol. Genom.* **2003**, *15*, 177–190, doi:10.1152/physiolgenomics.00062.2003.
33. Iacobas, D.A.; Iacobas, S.; Urban-Maldonado, M.; Scemes, E.; Spray, D.C. Similar transcriptomic alterations in Cx43 knock-down and knock-out astrocytes. *Cell Commun. Adhes* **2008**, *15*, 195–206, doi:10.1080/15419060802014222.
34. Surmiak M, Hubalewska-Mazgaj M, Wawrzycka-Adamczyk K, Musiał J, Sanak M. Delayed neutrophil apoptosis in granulomatosis with polyangiitis: dysregulation of neutrophil gene signature and circulating apoptosis-related proteins. *Scand J Rheumatol*. **2020**; 49(1):57-67. doi: 10.1080/03009742.2019.1634219. PMID: 31610684.
35. Zhao, Y.; Liu, X.; Zhong, L.; He, M.; Chen, S.; Wang, T.; Ma, S. The combined use of miRNAs and mRNAs as biomarkers for the diagnosis of papillary thyroid carcinoma. *Int J Mol Med* **2015**; 36(4):1097-103. doi: 10.3892/ijmm.2015.2305. PMID: 26252081.
36. Deligiorgi, M.V.; Mahaira, H,; Eftychiadis, C.; Kafiri, G,; Georgiou, G.; Theodoropoulos, G.; Konstadoulakis, M.M.;, Zografos, E.; Zografos, G.C. RANKL, OPG, TRAIL, KRas, and c-Fos expression in relation to central lymph node metastases in papillary thyroid carcinoma. *J BUON*. **2018,** 23(4):1029-1040. PMID: 30358208.
37. Kataki, A.; Sotirianakos, S.; Memos, N.; Karayiannis, M.; Messaris, E.; Leandros, E.; Manouras, A.; Androulakis, G. P53 and C-FOS overexpression in patients with thyroid cancer: an immunohistochemical study. *Neoplasma* **2003**; 50(1):26-30. PMID: 12687275.
38. Franceschi, S.; Lessi, F.; Panebianco, F.; Tantillo, E.; La Ferla, M.; Menicagli, M.; Aretini, P.; Apollo, A.; Naccarato, A.G.; Marchetti, I. et al. Loss of c-KIT expression in thyroid cancer cells. *PLoS One*. **2017**; 12(3):e0173913. doi: 10.1371/journal.pone.0173913. PMID: 28301608; PMCID: PMC5354407.
39. Chu, Y.H.; Sadow, P.M. Noninvasive follicular thyroid neoplasm with papillary-like nuclear features (NIFTP): Diagnostic updates and molecular advances. *Semin Diagn Pathol* **2020**, :S0740-2570(20)30058-7. doi: 10.1053/j.semdp.2020.06.001. PMID: 32646613.
40. Lubos, E.; Kelly, N.J.; Oldebeken, S.R.; Leopold, J.A.; Zhang, Y.Y.; Loscalzo, J.; Handy, D.E. Glutathione peroxidase-1 deficiency augments proinflammatory cytokine-induced redox signaling and human endothelial cell activation. *J Biol Chem*. **2011,** 14;286(41):35407-17. doi: 10.1074/jbc.M110.205708. PMID: 21852236; PMCID: PMC3195617.

41. Cardoso, M.F.S.; Castelletti, C.H.M.; Lima-Filho, J.L.; Martins, D.B.G.; Teixeira, J.A.C. Putative biomarkers for cervical cancer: SNVs, methylation and expression profiles. *Mutat Res*. **2017**; 773:161-173. doi: 10.1016/j.mrrev.2017.06.002PMID: 28927526.
42. Mei, L.; Shen, C.; Miao, R.; Wang, J.Z.; Cao, M.D.; Zhang, Y.S.; Shi, L.H.; Zhao, G.H.; Wang, M.H.; Wu, L.S. et al. RNA methyltransferase NSUN2 promotes gastric cancer cell proliferation by repressing p57Kip2 by an m5C-dependent manner. Cell Death Dis. 2020 Apr 24;11(4):270. doi: 10.1038/s41419-020-2487-z. PMID: 32332707; PMCID: PMC7181747.
43. Księżakowska-Łakoma, K.; Żyła, M.; Wilczyński, J.R. Mitochondrial dysfunction in cancer. *Prz Menopauzalny*. **2014**; 13(2):136-44. doi: 10.5114/pm.2014.42717. PMID: 26327844; PMCID: PMC4520353.
44. Huang, Y.P.; Chang, N.W. PPARα modulates gene expression profiles of mitochondrial energy metabolism in oral tumorigenesis. *Biomedicine (Taipei)*. **2016**; 6(1):3. doi: 10.7603/s40681-016-0003-7.
45. Roversi, F.M.; Olalla Saad, S.T.; Machado-Neto, J.A. Serine peptidase inhibitor Kunitz type 2 (SPINT2) in cancer development and progression. *Biomed Pharmacother*. **2018**, 101:278-286. doi: 10.1016/j.biopha.2018.02.100. PMID: 29499401.
46. Guan, X.; Guan, Z.; Song, C. Expression profile analysis identifies key genes as prognostic markers for metastasis of osteosarcoma. *Cancer Cell Int*. **2020**, 20:104. doi: 10.1186/s12935-020-01179-x. PMID: 32256213; PMCID: PMC7106759.
47. Graumann, J.; Finkernagel, F.; Reinartz, S.; Stief, T.; Brödje, D.; Renz, H.; Jansen, J.M.; Wagner, U.; Worzfeld, T.; Pogge von Strandmann, E.; et al. Multi-platform Affinity Proteomics Identify Proteins Linked to Metastasis and Immune Suppression in Ovarian Cancer Plasma. *Front Oncol*. **2019**, 9:1150. doi: 10.3389/fonc.2019.01150. PMID: 31737572; PMCID: PMC6839336.
48. Liu, F.; Cox, C.D.; Chowdhury, R.; Dovek, L.; Nguyen, H.; Li, T.; Li, S.; Ozer, B.; Chou, A.; Nguyen, N. et al. SPINT2 is hypermethylated in both IDH1 mutated and wild-type glioblastomas, and exerts tumor suppression via reduction of c-Met activation. *J Neurooncol*. **2019**, 142(3):423-434. doi: 10.1007/s11060-019-03126-x. Epub 2019 Mar 5. PMID: 30838489; PMCID: PMC6516751.
49. Pereira, M/S.; Celeiro, S.P.; Costa, Â.M.; Pinto ,F.; Popov, S.; de Almeida, G.C.; Amorim, J.; Pires, M.M.; Pinheiro, C.; Lopes, J.M. et al. Loss of SPINT2 expression frequently occurs in glioma, leading to increased growth and invasion via MMP2. *Cell Oncol* (Dordr). **2020**, 43(1):107-121. doi: 10.1007/s13402-019-00475-7. Epub 2019 Nov 7. PMID: 31701492.
50. Wu, L.; Shu, X.; Bao, J.; Guo, X.; Kote-Jarai, Z.; Haiman, C.A.; Eeles, R.A.; Zheng, W.; PRACTICAL, CRUK, BPC3, CAPS, PEGASUS Consortia. Analysis of Over 140,000 European Descendants Identifies Genetically Predicted Blood Protein Biomarkers Associated with Prostate Cancer Risk. *Cancer Res*. **2019**, 79(18):4592-4598. doi: 10.1158/0008-5472.CAN-18-3997. PMID: 31337649; PMCID: PMC6744971.
51. Ma, Z.; Liu, D.; Li, W.; Di, S.; Zhang, Z.; Zhang, J.; Xu, L.; Guo, K.; Zhu, Y.; Han, J. et al. STYK1 promotes tumor growth and metastasis by reducing SPINT2/HAI-2 expression in non-small cell lung cancer. *Cell Death Dis*. **2019**, 10(6):435. doi: 10.1038/s41419-019-1659-1. PMID: 31164631; PMCID: PMC6547759.
52. Roversi, F.M.; Cury, N.M.; Lopes, M.R.; Ferro, K.P.; Machado-Neto, J.A.; Alvarez, M.C,; Dos Santos, G.P.; Giardini Rosa, R.; Longhini, A.L.; Duarte, A.D.S.S. et al STO. Up-regulation of SPINT2/HAI-2 by Azacytidine in bone marrow mesenchymal stromal cells affects leukemic stem cell survival and adhesion. *J Cell Mol Med*. **2019**, 23(2):1562-1571. doi: 10.1111/jcmm.14066. PMID: 30484958; PMCID: PMC6349149.
53. Wang, N.; Che, Y.; Yin, F.; Yu, F.; Bi, X.; Wang, Y. Study on the methylation status of SPINT2 gene and its expression in cervical carcinoma. *Cancer Biomark*. **2018**; 22(3):435-442. doi: 10.3233/CBM-171050. PMID: 29843210.
54. Rodríguez, C.F.; Llorca, O. RPAP3 C-Terminal Domain: A Conserved Domain for the Assembly of R2TP Co-Chaperone Complexes. *Cells*. **2020**; 9(5):1139. doi: 10.3390/cells9051139. PMID: 32384603; PMCID: PMC7290369.
55. Kawachi, T.; Tanaka, S.; Fukuda, A.; Sumii, Y.; Setiawan, A.; Kotoku, N.; Kobayashi, M.; Arai, M. Target Identification of the Marine Natural Products Dictyoceratin-A and -C as Selective Growth Inhibitors in Cancer Cells Adapted to Hypoxic Environments. *Mar Drugs*. **2019**; 17(3):163. doi: 10.3390/md17030163. PMID: 30857246; PMCID: PMC6471994.
56. Liu, F.; Zhao, H.; Gong, L.; Yao, L.; Li, Y.; Zhang, W. MicroRNA-129-3p functions as a tumor suppressor in serous ovarian cancer by targeting BZW1. *Int J Clin Exp Pathol*. **2018**; 11(12):5901-5908. PMID: 31949677; PMCID: PMC6963061.

57. Chiou, J.; Chang, Y.C.; Jan, Y.H.; Tsai, H.F.; Yang, C.J.; Huang, M.S.; Yu, Y.L.; Hsiao, M. Overexpression of BZW1 is an independent poor prognosis marker and its down-regulation suppresses lung adenocarcinoma metastasis. *Sci Rep*. **2019**; 9(1):14624. doi: 10.1038/s41598-019-50874-x. PMID: 31601833; PMCID: PMC6786993.
58. Li, S.; Chai, Z.; Li, Y.; Liu, D.; Bai, Z.; Li, Y.; Li, Y.; Situ, Z. BZW1, a novel proliferation regulator that promotes growth of salivary muocepodermoid carcinoma. *Cancer Lett*. **2009**; 284(1):86-94. doi: 10.1016/j.canlet.2009.04.019. PMID: 19446954.
59. Iacobas, D.A.; Iacobas, S.; Spray, D.C. Connexin-dependent transcellular transcriptomic networks in mouse brain. *Prog Biophys Mol Biol* **2007**, 94(1-2):168-184. Review. DOI:10.1016/j.pbiomolbio.2007.03.015. PMID:17507080.